# Enhancer RNA-based modeling of adverse events and objective responses of immunotherapy

Mengbiao Guo[1,*], Zhiya Lu[1,*], Yuanyan Xiong[1,#]

[1] Key Laboratory of Gene Engineering of the Ministry of Education, Institute of Healthy Aging Research, School of Life Sciences, Sun Yat-sen University, Guangzhou 510006, China.

[*] These authors contributed equally to this work.

[#] Corresponding author: xyyan@mail.sysu.edu.cn, Tel: +86-20-39943531, Fax: +86-20-39943778

## Abstract

Immune checkpoint inhibitors (ICI) targeting PD-1/PD-L1 or CTLA-4 are emerging and effective immunotherapy strategies. However, ICI treated patients present heterogeneous responses and adverse events, thus demanding effective ways to assess benefit over risk before treatment. Here, by integrating pan-cancer clinical and molecular data, we tried to predict immune-related adverse events (irAEs, risk) and objective response rates (ORRs, benefit) based on enhancer RNAs (eRNAs) expression among patients receiving anti-PD-1/PD-L1 therapy. We built two effective regression models, explaining 71% variance (R=0.84) of irAEs with three eRNAs and 79% (R=0.89) of ORRs with five eRNAs. Interestingly, target genes of irAE-related enhancers, including upstream regulators of MYC, were involved in metabolism, inflammation, and immune activation, while ORR-related enhancers target *PAK2* and *DLG1* which directly participate in T cell activation. Our study provides references for the

identification of immunotherapy-related biomarkers and potential therapeutic targets during immunotherapy.

## Introduction

Immune checkpoints (ICs) generally refer to key inhibitory factors of the immune system, including programmed cell death 1 (PD-1 or CD279) and its ligand programmed cell death 1 ligand 1 (PD-L1 or CD274) that control the T cell response and fate during tumor immunity [1]. In tumor samples, PD-1 and PD-L1 mainly expressed in T cells and tumor cells, respectively, and tumors exploit their interaction to escape the immune system by counteracting the stimulatory signals from the interaction between T cell receptor (TCR) and major histocompatibility complex (MHC) and other costimulatory signals [2-4].

PD-1/PD-L1 has been translated to the clinical practice, and ICI treatment targeting PD-1/PD-L1 proved to offer significant clinical benefits in many cancers, with an ORR from 20% to 50% in multiple clinical trials and for various types of cancer [5]. However, only a small subset of patients showed long-lasting remission, despite remarkable benefits of ICI therapies. Patients of some cancers were completely refractory to checkpoint blockade, occasionally leading to considerable side effects. To predict treatment benefit, PD-L1 expression was proposed as the first biomarker of anti–PD-1/PD-L1 therapy effectiveness [6], followed by tumor mutational burden (TMB) [7]. Later, microsatellite instability (MSI) [8], CD8+ T-cell abundance [9, 10], cytolytic activity [11], and intestinal microbial composition[12] were proposed to prioritize patients with potentially more treatment gains.

On the other hand, irAEs result from excessive immunity against normal organs. Most studies show that the incidence of irAEs caused by anti-PD-1/PD-L1 treatment is about 60% [13, 14]. Although nearly all organs can be affected, irAEs mostly involved the gastrointestinal tract, endocrine glands, skin, and liver [15]. In some cases, irAE can be lethal. For example, pneumonitis is the most common fatal irAE with a 10% death rate, accounting for 35% of anti-PD-1/PD-L1-related fatalities [16]. The mortality of myocarditis, the most lethal irAE, could even reach about 50% [17]. Therefore, it is important and urgent to select patients with potentially significant benefit over risk of ICI treatments based on individual molecular data. Although people have discovered several predictors of irAEs using expression of protein-coding genes [18], studying irAE-related non-coding elements would probably provide a better mechanistic understanding of why PD-1/PD-L1 pathway modulation leads to significant clinical benefit in some patients but temporary, partial, or no clinical benefit in other patients.

Recent studies found that eRNAs (non-coding RNAs) were usually transcribed from active enhancers and eRNA levels portended enhancer activities across tissues [19]. Numerous cancer-associated eRNAs have been identified and eRNAs were proposed as potential therapeutic targets [20]. Here, we comprehensively investigate the adverse events and the response rates in patients receiving anti-PD-1/PD-L1 therapies across cancer types. By integrating clinical data and molecular data, we identify predictors based on three eRNAs for predicting irAE and five eRNAs for ORR. Further exploring enhancer-target interaction identified functional genes that may help explain the overall risk or benefit of anti-PD-1/PD-L1 therapy, including MLXIPL, RAF1, MPL, PAK2, DLG1. In summary, our study reveals potential mechanisms underlying ICI therapy based on enhancer activity.

# Results

## Three eRNAs effectively predict irAE of immunotherapy

To identify factors to predict irAEs, we first examined correlations between 7 045 eRNAs and irAE RORs across 25 cancer types and found 178 eRNAs positively correlated with irAEs with nominal significance ($P$<0.05). Among these eRNAs, ENSR00000041252 showed the highest correlation (correlation R=0.68, $P$=1.6e-4; **Fig. S1A**), stronger than immune factors, including naive B cells, CD8+ T cells, macrophages M1, and T cell receptor diversity [18].

Then, we selected the top ten eRNAs (**Table S1**) to build prediction models. Multicollinearity analysis resulted in six roughly independent eRNAs, ENSR00000041252, ENSR00000326714, ENSR00000148786, X14.65054944.65060944, ENSR00000118775, and ENSR00000242410 (**Fig. 1A** and **Fig. 1B**). Next, we obtained 15 significant bivariate regression models using the irAE-correlated enhancers. Correlation between the observed and predicted irAE ROR values showed that the combination ENSR00000148786 + ENSR00000005553 achieved the best predictive performance (R=0.79, $P$=3.1e-6; **Fig. S1B**). Further increasing model factors resulted in the optimal tri-variate model, ENSR00000041252 + ENSR00000148786 + ENSR00000005553, with the strongest correlation (R=0.84, $P$=2.1e-6; **Fig. 1C**). Of note, no improvement was observed after adding the two protein-coding genes (LCP1 and ADPGK) from a model reported previously [18], suggesting the independence of our model. Although showing slightly lower performance than the previous protein-coding gene model (LCP1+ADPGK), our enhancer-based model, explaining 71% (R-squared, R=0.84) of irAE variance, demonstrated that eRNAs alone can effectively predict irAEs.

## Five eRNAs effectively predict immunotherapy benefit

Similarly, to identify factors to predict ORRs, we identified 28 out of 7 045 eRNAs positively correlated with ORR ($P$<0.05; the best one ENSR00000187665 shown in **Fig. S1C**). Based on the top ten eRNAs (**Table S2**), after multicollinearity analysis (**Fig. 1D** and **Fig. 1E**), two bivariate models achieved better predictive performance than single-eRNA models (one shown in **Fig. S1D**; R=0.82, $P$=2.0e-5). Further adding model factors resulted in four equally-efficient optimal trivariate models (involving five key eRNAs, **Table S3**) for ORR prediction were able to effectively predict the efficacy of anti–PD-1/PD-L1 treatments. One example, ENSR00000164478 + ENSR00000035913+ ENSR00000167231, was shown in **Fig. 1F** (R=0.89, $P$=3.3e-7).

**Enhancer-target networks of irAE and ORR-associated enhancers**

Enhancers were assumed to affect irAEs or ORRs by activating target genes through long-range interactions. We downloaded enhancer-target interaction data[21] and obtained putative targets of our enhancers. Two eRNAs (ENSR00000262415 and ENSRO0000167231) were excluded from downstream analysis due to lack of any annotated target gene. eRNA-target networks showed that these enhancers independently regulated a specific groups of targets (**Fig. 2A** and **Fig. 2B**, note that ENSR00000164478 and ENSR00000164479 located to the same genomic region), indicating that each irAE-related enhancer was involved in different regulatory modules. Similarly, protein-protein interaction (PPI) analysis revealed that an independent network was controlled by each enhancer (**Fig. 1C** and **Fig. 1D**). In these PPI networks, genes located in the center (such as BCL7B, TBL2, and NAP1L4) might be vital regulators of irAEs or ORRs.

**Enhancer targets reveal metabolic and inflammatory genes involved in irAEs**

Next, we downloaded gene sets from COSMIC[22] and oncoKB[23] and examined our eRNA targets in known oncogenic signaling pathways using cBioPortal[24, 25]. We found that some eRNA targets were known cancer genes relevant to tumor immunity, including *MLXIPL, MPL, RAF1*, and *XPC*. *RAF1* was annotated as an oncogene and participated in the RTK-RAS signaling pathway (**Fig. S2A**) and MLXIPL was involved in MYC signaling pathway (**Fig. S2B**). A previous work[26] shows RAF1 can activate MAPK1 and NF-κB pathways to regulate genes involved in inflammation. Therefore, RAF1 may enhance immunoreaction and subsequently cause irAEs via Natural Killer cell-mediated cytotoxicity, T cell receptor signaling pathway, and B cell receptor signaling pathway.

Interestingly, we found that ENSR00000326714 targets were enriched in a large number of metabolic and biosynthesis processes (**Fig. 2E**). This was reminiscent of some types of adverse events, such as diabetes[16], due to metabolic disturbances or metabolic disorders. Specifically, the core network of ENSR00000326714 targets consists of seven metabolic and inflammatory genes, namely, BAZ1B, BCL7B, TBL2, MLXIPL, NSUN, STX1A, and VPS37D. Among them, BAZ1B, BCL7B, TBL2 and MLXIPL are pleiotropic genes for lipids and inflammatory markers in the liver[27]. Of note, MLXIPL encodes the carbohydrate-responsive element-binding protein (ChREBP), which mediates glucose homeostasis and liver lipid metabolism. ChREBP was also associated with up-regulation of several cytokines (TNF-α, IL-1β, and IL-6) in patients with type 2 diabetes mellitus, promoting the inflammatory responses and apoptosis of mesangial cells[28]. STX1A encodes a member of the syntaxin superfamily, syntaxin 1A. It contributes to neural function in the central nervous system by regulating transmitter release[29]. As a kind of target-SNAP receptor (t-SNAREs), it is involved in insulin exocytosis[30]. Severely reduced islet syntaxin 1A level was reported to contribute to insulin

149 secretory deficiency[31]. Given that diabetes and hepatitis account for ~30% of immune-
150 related adverse events[16], we speculate that ENSR00000326714 augmented the expression of
151 the these genes, subsequently triggering inflammation and other toxic effects on these patients.
152
153 **ORR enhancers reveal immune activation genes for immunotherapy benefit**
154
155 We also analyzed target genes of ORR-predictable eRNAs (**Fig. 2B**), which included three
156 types of genes. PAK2, LMLN, DLG1, ASCL2, SENP5, IQCG, and BRSK2 are related to cell
157 cycle, cell division, and differentiation. PIGZ, PIGX, PCYT1A, CARS, and BDH1 are
158 metabolic genes; TRPM5, KCNQ1, and FYTTD1 are responsible for cellular transport and
159 signal transduction. In particular, target genes of ORR-related ENSR00000164478 were
160 enriched in glycosylphosphatidylinositol (GPI)-anchor biosynthesis (FDR=$4.73\times10^{-3}$) (**Fig. 2F**)
161 and T-cell receptor signaling (FDR=$3.78\times10^{-2}$), among other enriched pathways (**Fig. 2G**).
162
163 Furthermore, PAK2 and DLG1 directly took part in the T cell activation pathway, which
164 explains their connection with ORR. P21 (RAC1) activated kinase 2 (PAK2) has been reported
165 as a key signaling molecule in the differentiation of T cells. PAK2 is essential in T cell
166 development and differentiation[32], indicating its potential function in T cell-initiated
167 autoimmunity. DLG1 encodes a multi-domain scaffolding protein from the membrane-
168 associated guanylate kinase family, which has been shown to regulate the antigen receptor
169 signaling and cell polarity in lymphocytes, involved in activation and proliferation of T cells[33,
170 34]. Our results provide more support for the T cells as the regulators in immune responses
171 during immune checkpoint blockade therapy.
172 Lastly, PIGZ encodes a protein that is previously identified as an immune-associated prognosis
173 signature[35]. However, knowledge of the relationship between PIGZ and the immune system

is still poorly established. The association between PIGZ expression and immune benefits during anti-PD1/PDL1 immunotherapy needs further elucidation.

## Discussions

In this work, we presented a preliminary evaluation of the different enhancer-target interactions associated with anti–PD-1/PD-L1 immunotherapy across tumor types, and successfully identify potential enhancer-based biomarkers of risk and beneficial response. We suggest that, during immunotherapy, enhanced expression of inflammatory factors including MLXIPL, STX1A, and RAF1 may lead to a higher risk of irAEs, while strengthening immune activation factors including PAK2 and DLG1 may improve anti-tumor immunity. Besides, we discovered many other cancer-related, metabolic, signaling or regulatory genes possess predictive potential, which warrants further investigation.

Several limitations remain for future work and our results need to be carefully interpreted. First, the majority of data are collected from previous individual studies[21], introducing inherent limitations of their work. Second, there are inevitable flaws of modeling as well, due to the low expression level of eRNA and small sample size. The overall quality of predictive models of ORR is inferior to those of irAEs, probably due to a smaller sample size as well as larger sparsity of ORR data. Finally, since results in this project are mainly based on computational predictions and the support of existing literature, our findings need further experimental validation. A larger dataset is required to comprehensively model side effects or immune response as well.

# Methods

## Data collection

To quantify the risk of immune-related adverse events (irAEs), reporting odds ratio (ROR) was calculated as previously described [36]. The anti-PD1/PD-L1 irAE ROR and ORR values across different cancer types were collected from previous studies [10, 18]. RNA-seq expression data (RSEM normalized counts, log2-transformed) across 25 TCGA cancers were downloaded from the UCSC Xena platform (http://xena.ucsc.edu/). Expression levels of selected genes were extracted for downstream analysis, and the average value was calculated for each TCGA cohort. We downloaded eRNA expression levels and enhancer-target associations for 7 045 enhancer RNAs in ~7,300 samples from the eRic database [21] (https://hanlab.uth.edu/eRic/). Mean eRNA expression (log2-transformed RPM values) were used. Similar to gene expression, we averaged the expression level of each eRNA for each cancer.

## Prediction model construction

First, the top ten eRNAs were selected based on correlation between eRNA and irAE or ORR. Before constructing bivariate models, the variance inflation factor[37] (VIF) of these ten eRNAs was calculated to evaluate the multicollinearity. Generally, we set the threshold of VIF value to 4 (a VIF value greater than 10 will be considered serious multicollinearity). The optimal prediction model was obtained by step-wise addition of model factors (eRNA) and evaluate the correlation between predicted and observed patient risk or benefits.

## Bioinformatics tools

We used the protein-protein interaction (PPI) database STRING[38] (v11, https://string-db.org) to investigate selected eRNA target genes. Basic GO and KEGG term enrichment and visualization were conducted with the R package clusterProfiler[39] (v3.14.3). Extensive functional annotation of eRNA target genes were performed with DAVID [40] (v6.8) (https://david.ncifcrf.gov/). To verify cancer-related function for genes of interest, a credible set of 723 cancer genes was downloaded from the Cancer Gene Census (CGC) project of the COSMIC[22] repository (https://cancer.sanger.ac.uk/cosmic/). Another database oncoKB[23] (https://oncokb.org/), which has a list of 1,064 cancer genes, was added as a supplement to COSMIC CGC genes. Oncogenic signaling pathways were provided by the cBioPortal database[24] (http://www.cbioportal.org/). Statistical analysis and visualization were performed in R (v3.6.3) using packages ggplot2 (v3.3.2), networkD3 (v0.4). For novel candidates, we used three types of biological interpretation (Gene Oncology, Pathways, and Protein-Protein Interaction) to obtain biological knowledge.

**Statistical methods**

We employed an approach as described previously [10, 18] to evaluate the correlation between eRNAs and irAE RORs or ORRs. Linear-regression models for predicting irAE ROR or ORR across cancer types, was constructed by the R function lm, and the performance of the prediction was estimated based on Spearman rank correlation, using the R package psych (v2.0.12). To compare the goodness of fit between different models, a log-likelihood ratio test was performed using the R package lmtest (v0.9). We compute variance inflation factor (VIF) to assess multicollinearity using the vif function from the R package car (v3.0) to exclude combinations containing highly correlated factors.

## Acknowledgements

The research has been supported by National Natural Science Foundation of China (NSFC) (Grant 31571350, U1611265, and 31871323). The results shown here are in whole or part based upon data generated by the TCGA or CPTAC Research Network.

## Conflict of Interests

The authors declare no competing interests.

## Author contributions

YYX and MBG conceived and supervised the study. ZYL, YYX, and MBG performed the analysis. MBG drafted the manuscript with assistance from ZYL. YYX reviewed the manuscript. All authors approved the final manuscript.

## References

1 Boussiotis VA. Molecular and Biochemical Aspects of the PD-1 Checkpoint Pathway. *N Engl J Med* 2016; 375: 1767-1778.

2 Dong H, Strome SE, Salomao DR, Tamura H, Hirano F, Flies DB *et al*. Tumor-associated B7-H1 promotes T-cell apoptosis: a potential mechanism of immune evasion. *Nat Med* 2002; 8: 793-800.

3 Sharpe AH, Pauken KE. The diverse functions of the PD1 inhibitory pathway. *Nat Rev Immunol* 2018; 18: 153-167.

4 Keir ME, Butte MJ, Freeman GJ, Sharpe AH. PD-1 and its ligands in tolerance and immunity. *Annu Rev Immunol* 2008; 26: 677-704.

5 Topalian SL, Hodi FS, Brahmer JR, Gettinger SN, Smith DC, McDermott DF *et al*. Safety, activity, and immune correlates of anti-PD-1 antibody in cancer. *N Engl J Med* 2012; 366: 2443-2454.

6 Patel SP, Kurzrock R. PD-L1 Expression as a Predictive Biomarker in Cancer Immunotherapy. *Mol Cancer Ther* 2015; 14: 847-856.

7 Yarchoan M, Hopkins A, Jaffee EM. Tumor Mutational Burden and Response Rate to PD-1 Inhibition. *N Engl J Med* 2017; 377: 2500-2501.

8 Le DT, Durham JN, Smith KN, Wang H, Bartlett BR, Aulakh LK *et al*. Mismatch repair deficiency predicts response of solid tumors to PD-1 blockade. *Science* 2017; 357: 409-413.

9 Yu X, Zhang Z, Wang Z, Wu P, Qiu F, Huang J. Prognostic and predictive value of tumor-infiltrating lymphocytes in breast cancer: a systematic review and meta-analysis. *Clin Transl Oncol* 2016; 18: 497-506.

10 Lee JS, Ruppin E. Multiomics Prediction of Response Rates to Therapies to Inhibit Programmed Cell Death 1 and Programmed Cell Death 1 Ligand 1. *JAMA Oncol* 2019.

11 Rooney MS, Shukla SA, Wu CJ, Getz G, Hacohen N. Molecular and genetic properties of tumors associated with local immune cytolytic activity. *Cell* 2015; 160: 48-61.

12 Pitt JM, Vetizou M, Daillere R, Roberti MP, Yamazaki T, Routy B *et al*. Resistance Mechanisms to Immune-Checkpoint Blockade in Cancer: Tumor-Intrinsic and -Extrinsic Factors. *Immunity* 2016; 44: 1255-1269.

13 Chow LQM, Haddad R, Gupta S, Mahipal A, Mehra R, Tahara M *et al*. Antitumor Activity of Pembrolizumab in Biomarker-Unselected Patients With Recurrent and/or Metastatic Head and Neck Squamous Cell Carcinoma: Results From the Phase Ib KEYNOTE-012 Expansion Cohort. *J Clin Oncol* 2016; 34: 3838-3845.

14 Zandberg DP, Algazi AP, Jimeno A, Good JS, Fayette J, Bouganim N *et al*. Durvalumab for recurrent or metastatic head and neck squamous cell carcinoma: Results from a single-arm, phase II study in patients with >/=25% tumour cell PD-L1 expression who have progressed on platinum-based chemotherapy. *Eur J Cancer* 2019; 107: 142-152.

15 Weber JS, Hodi FS, Wolchok JD, Topalian SL, Schadendorf D, Larkin J *et al*. Safety Profile of Nivolumab Monotherapy: A Pooled Analysis of Patients With Advanced Melanoma. *J Clin Oncol* 2017; 35: 785-792.

16 Wang DY, Salem JE, Cohen JV, Chandra S, Menzer C, Ye F *et al*. Fatal Toxic Effects Associated With Immune Checkpoint Inhibitors: A Systematic Review and Meta-analysis. *JAMA Oncol* 2018; 4: 1721-1728.

17 Salem JE, Manouchehri A, Moey M, Lebrun-Vignes B, Bastarache L, Pariente A *et al*. Cardiovascular toxicities associated with immune checkpoint inhibitors: an observational, retrospective, pharmacovigilance study. *Lancet Oncol* 2018; 19: 1579-1589.

18 Jing Y, Liu J, Ye Y, Pan L, Deng H, Wang Y *et al*. Multi-omics prediction of immune-related adverse events during checkpoint immunotherapy. *Nat Commun* 2020; 11: 4946.

19 Andersson R, Gebhard C, Miguel-Escalada I, Hoof I, Bornholdt J, Boyd M *et al*. An atlas of active enhancers across human cell types and tissues. *Nature* 2014; 507: 455-461.

20 Leveille N, Melo CA, Agami R. Enhancer-associated RNAs as therapeutic targets. *Expert Opin Biol Ther* 2015; 15: 723-734.

21 Zhang Z, Lee JH, Ruan H, Ye Y, Krakowiak J, Hu Q *et al*. Transcriptional landscape and clinical utility of enhancer RNAs for eRNA-targeted therapy in cancer. *Nat Commun* 2019; 10: 4562.

22 Tate JG, Bamford S, Jubb HC, Sondka Z, Beare DM, Bindal N *et al*. COSMIC: the Catalogue Of Somatic Mutations In Cancer. *Nucleic Acids Res* 2019; 47: D941-D947.

23 Chakravarty D, Gao J, Phillips SM, Kundra R, Zhang H, Wang J *et al*. OncoKB: A Precision Oncology Knowledge Base. *JCO Precis Oncol* 2017; 2017.

24 Cerami E, Gao J, Dogrusoz U, Gross BE, Sumer SO, Aksoy BA *et al*. The cBio cancer genomics portal: an open platform for exploring multidimensional cancer genomics data. *Cancer Discov* 2012; 2: 401-404.

25 Gao J, Aksoy BA, Dogrusoz U, Dresdner G, Gross B, Sumer SO *et al*. Integrative analysis of complex cancer genomics and clinical profiles using the cBioPortal. *Sci Signal* 2013; 6: pl1.

26 Lappas M. RAF1 is increased in labouring myometrium and modulates inflammation-induced pro-labour mediators. *Reproduction* 2016; 151: 411-420.

27 Kraja AT, Chasman DI, North KE, Reiner AP, Yanek LR, Kilpelainen TO *et al*. Pleiotropic genes for metabolic syndrome and inflammation. *Mol Genet Metab* 2014; 112: 317-338.

28 Chen Y, Wang YJ, Zhao Y, Wang JC. Carbohydrate response element binding protein (ChREBP) modulates the inflammatory response of mesangial cells in response to glucose. *Biosci Rep* 2018; 38.

29 Fujiwara T, Kofuji T, Akagawa K. Dysfunction of the hypothalamic-pituitary-adrenal axis in STX1A knockout mice. *J Neuroendocrinol* 2011; 23: 1222-1230.

30 Bagge A, Dahmcke CM, Dalgaard LT. Syntaxin-1a is a direct target of miR-29a in insulin-producing beta-cells. *Horm Metab Res* 2013; 45: 463-466.

31 Liang T, Qin T, Xie L, Dolai S, Zhu D, Prentice KJ *et al*. New Roles of Syntaxin-1A in Insulin Granule Exocytosis and Replenishment. *J Biol Chem* 2017; 292: 2203-2216.

32 Phee H, Au-Yeung BB, Pryshchep O, O'Hagan KL, Fairbairn SG, Radu M *et al*. Pak2 is required for actin cytoskeleton remodeling, TCR signaling, and normal thymocyte development and maturation. *Elife* 2014; 3: e02270.

33 Gmyrek GB, Graham DB, Sandoval GJ, Blaufuss GS, Akilesh HM, Fujikawa K *et al*. Polarity gene discs large homolog 1 regulates the generation of memory T cells. *Eur J Immunol* 2013; 43: 1185-1194.

34 Dong X, Li X, Liu C, Xu K, Shi Y, Liu W. Discs large homolog 1 regulates B-cell proliferation and antibody production. *Int Immunol* 2019; 31: 759-770.

389 35 Hu B, Yang XB, Sang XT. Development and Verification of the Hypoxia-Related and
390 Immune-Associated Prognosis Signature for Hepatocellular Carcinoma. *J Hepatocell*
391 *Carcinoma* 2020; 7: 315-330.
392
393 36 Bate A, Evans SJ. Quantitative signal detection using spontaneous ADR reporting.
394 *Pharmacoepidemiol Drug Saf* 2009; 18: 427-436.
395
396 37 Oshima Y, Tanimoto T, Yuji K, Tojo A. EGFR-TKI-Associated Interstitial
397 Pneumonitis in Nivolumab-Treated Patients With Non-Small Cell Lung Cancer.
398 *JAMA Oncol* 2018; 4: 1112-1115.
399
400 38 Szklarczyk D, Gable AL, Lyon D, Junge A, Wyder S, Huerta-Cepas J *et al*. STRING
401 v11: protein-protein association networks with increased coverage, supporting
402 functional discovery in genome-wide experimental datasets. *Nucleic Acids Res* 2019;
403 47: D607-D613.
404
405 39 Yu G, Wang LG, Han Y, He QY. clusterProfiler: an R package for comparing
406 biological themes among gene clusters. *OMICS* 2012; 16: 284-287.
407
408 40 Huang da W, Sherman BT, Lempicki RA. Systematic and integrative analysis of large
409 gene lists using DAVID bioinformatics resources. *Nat Protoc* 2009; 4: 44-57.
410
411
412

# Figure Legends

**Fig. 1**

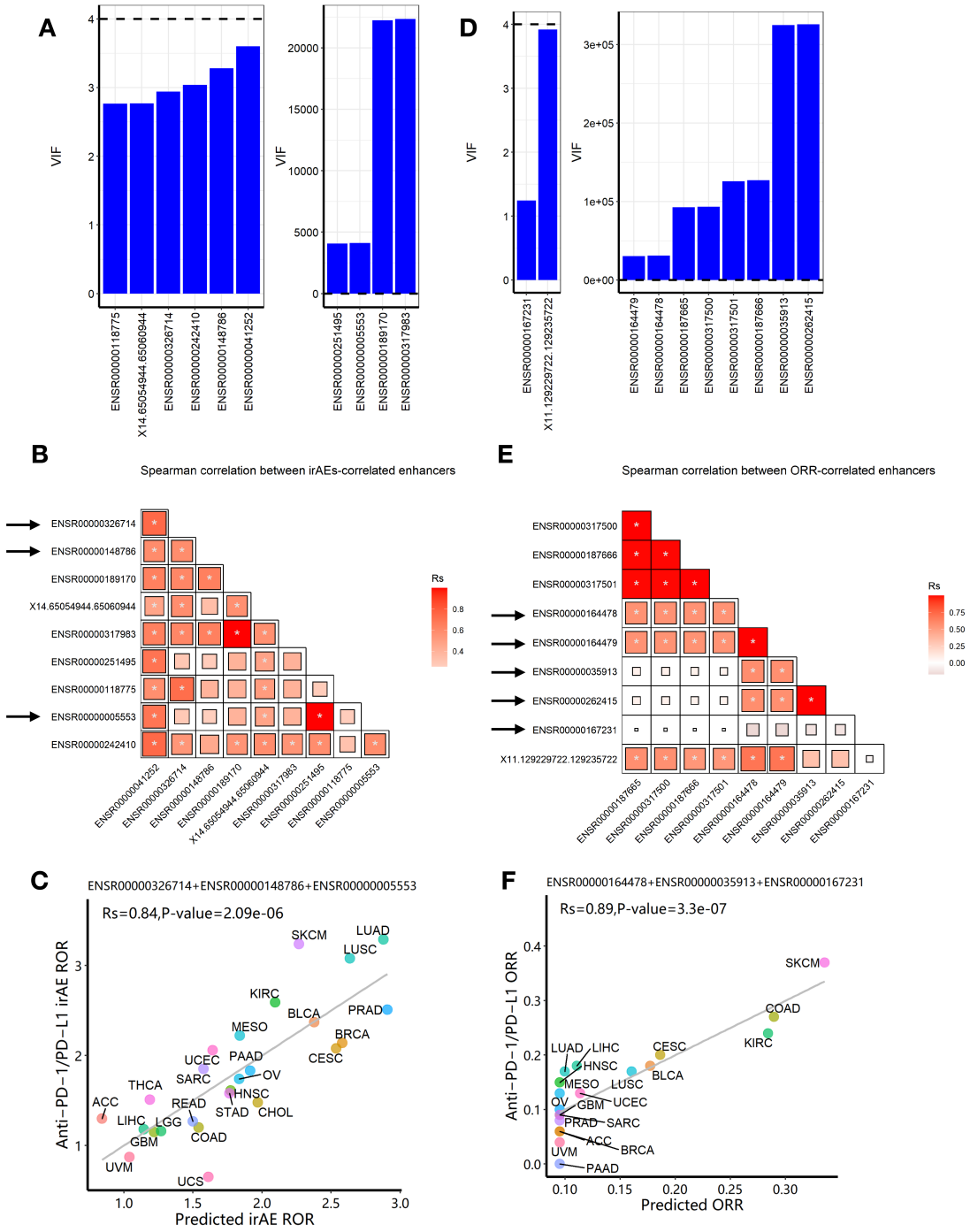


**Fig.1, Construction of eRNA-based prediction models for irAE ROR (risk) and ORR (benefit) of immunotherapy.** (**A**) Multicollinearity (VIF) analysis for top ten eRNA expression in predicting irAEs. Six eRNAs showed no multicollinearity, while 4 eRNAs

showed strong multicollinearity. (**B**) Spearman correlation between irAE-correlated eRNAs. Pairwise Spearman correlation (Rs) of expression level between candidate eRNAs. The shade of the square indicates the Rs, and the size indicates P-value (* indicates statistical significance $P < 0.05$). (**C**) Combined effect of ENSR00000326714, ENSR00000148786 and ENSR00-000005553 trivariate model of predicting irAEs (R=0.84, *P*=2.1e-6). The equation of the best trivariate model is 0.1912*ENSR00000005553+0.4097*ENSR000-00326714+0.1953*ENSR00000148786+0.2942. (**D**) Multicollinearity analysis for top ten eRNA expression in predicting ORR. Two eRNAs showed no multicollinearity, while 8 eRNAs showed strong multicollinearity. (**E**) Spearman correlation between ORR-correlated eRNAs. Spearman correlation (*Rs*) of expression level was calculated between two candidate eRNAs. The shade of the square indicates the *Rs*, and the size indicates P-value (* indicates statistical significance $P< 0.05$). (**F**) Combined effect of ENSR00000164478, ENSR00000035913 and ENSR000-00167231 trivariate model of predicting ORR (R=0.89, *P*=3.3e-7). The equation of the best trivariate model is 0.0953+0.0649* ENSR00000164478+0.0032* ENSR00000035913+0.1687* ENSR00000167231. irAE, immune-related adverse events; ROR, reporting odds ratio; ORR, objective response rates; LUAD, lung adenocarcinoma; SKCM, skin cutaneous melanoma; LUSC, lung squamous cell carcinoma; KIRC, kidney renal clear cell carcinoma; PRAD, prostate adenocarcinoma; BLCA, bladder urothelial carcinoma; MESO, mesothelioma; BRCA, breast invasive carcinoma; CESC, cervical squamous cell carcinoma and endocervical adenocarcinoma; UCEC, uterine corpus endometrial carcinoma; SARC, sarcoma; ESCA, esophageal carcinoma; PAAD, pancreatic adenocarcinoma; OV, ovarian serous cystadenocarcinoma; HNSC, head and neck squamous cell carcinoma; STAD, stomach adenocarcinoma; THCA, thyroid carcinoma; CHOL, cholangiocarcinoma; ACC, adrenocortical carcinoma; READ, rectum adenocarcinoma; COAD,

442 colon adenocarcinoma; LIHC, liver hepatocellular carcinoma; LGG, brain lower-grade glioma;

443 GBM, glioblastoma multiforme; UVM, uveal melanoma; UCS, uterine carcinosarcoma.

444

**Fig. 2**

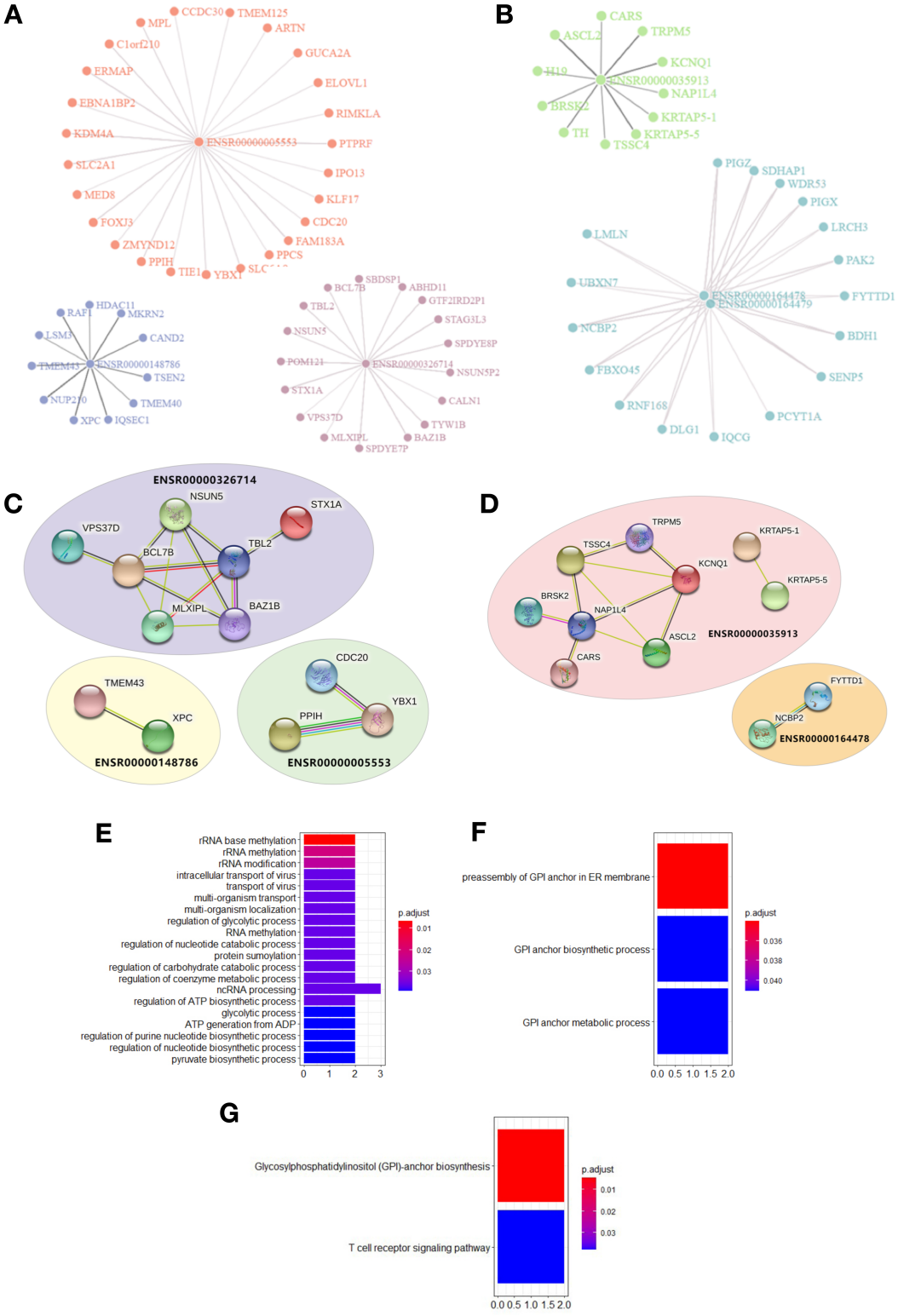

**Fig. 2.** Visualization of enhancer-target interaction network and functional enrichment. **(A)** target genes of irAE-related enhancers ENSR00000005553, ENSR00000326714, and ENSR00000148786. **(B)** target genes of ORR-related enhancers ENSR00000164478, ENSR00000164479, and ENSR00000035913. (**C**) Protein-Protein Interaction (PPI) network for target genes of irAE-related enhancer ENSR00000326714, ENSR00000148786, ENSR00000005553; and their corresponding PPI of targets in irAE ROR model. **(D)** PPI network for targets of ORR-related enhancers ENSR00000035913, ENSR000-00164478. (**E**) GO enrichment of genes regulated by irAE-correlated enhancer ENSR00000326714. (**F**) GO enrichment of genes regulated by ORR-correlated enhancer ENSR00000164478. (**G**) KEGG pathway enrichment of genes regulated by ORR-correlated enhancer ENSR00000164478.